arXiv:1602.01813v1 [cond-mat.mtrl-sci] 2 Feb 2016

Linewidths in excitonic absorption spectra of cuprous oxide

Frank Schweiner, Jörg Main, and Günter Wunner
Institut für Theoretische Physik 1, Universität Stuttgart, 70550 Stuttgart, Germany
(Dated: February 5, 2016)

We present a theoretical calculation of the absorption spectrum of cuprous oxide (Cu_2O) based on the general theory developed by Y. Toyozawa. An inclusion not only of acoustic phonons but also of optical phonons and of specific properties of the excitons in Cu_2O like the central-cell corrections for the $1S$-exciton allows us to calculate the experimentally observed line widths in experiments by T. Kazimierczuk *et al* [Nature **514**, 343, (2014)] within the same order of magnitude, which demonstrates a clear improvement in comparison to earlier work on this topic. We also discuss a variety of further effects, which explain the still observable discrepancy between theory and experiment but can hardly be included in theoretical calculations.

PACS numbers: 71.35.-y, 63.20.-e

I. INTRODUCTION

Ever since the first formulation of their concept by Frenkel [1–3], Peierls [4], and Wannier [5] in the 1930s, and their experimental discovery in cuprous oxide (Cu_2O) by Gross and Karryjew in 1952 [6], excitons are of large physical interest, because they are the quanta of the fundamental optical excitations in both insulators and semiconductors in the visible and ultraviolet spectrum of light. Excitons are so-called quasi-particles being composed of an electron and a positivley charged hole. Wannier excitons extend over many unit cells of the crystal and can be treated within a very simple approach as an analogue of the hydrogen atom. The corresponding Schrödinger equation, which describes these excitons, is the so-called Wannier equation [7–9].

Very recently, the hydrogen-like series could be observed experimentally for the so-called yellow exciton in Cu_2O for the first time up to a large principal quantum number of $n = 25$ [10]. This detection has brought new interest to the field of excitons [11–14]. However, the line widths detected in Ref. [10] differ from earlier theoretical calculations on this topic [15], which leads us to a new investigation of the main parameters describing the shape of the excitonic absorption lines.

The main features, which make Cu_2O one of the most investigated semiconductors relating to excitons, are the large excitonic binding energy of $R_{\mathrm{exc}} \approx 86\,\mathrm{meV}$ [11] and the non-degeneracy of its uppermost valence band justifying the simple-band model with a hydrogen-like exciton spectrum

$$E_{n\boldsymbol{K}} = E_{\mathrm{gap}} - \frac{R_{\mathrm{exc}}}{n^2} + \frac{\hbar^2 \boldsymbol{K}^2}{2M}. \tag{1}$$

Besides the band gap energy E_{gap}, we also include the energy due to a finite momentum $\hbar\boldsymbol{K}$ of the center of mass. By M we denote the mass of the exciton in effective-mass approximation. Beyond the simple-band model, one often has to account for a variety of further effects of the solid. Possible corrections of this model include, e.g., central-cell corrections [16], a coupling of the uppermost valence band to other valence bands [13, 17], and especially the interaction with phonons, which are the quasiparticles of lattice vibrations. This interaction is, besides the effect of impurities in the crystal, the main cause for an asymmetric broadening and shifting of the excitonic lines observed in absorption spectra [8]. The general theory for the effect of phonons on excitonic spectra has been developed by Toyozawa in the late 1950s and early 1960s [15, 18–20].

In the following we will apply the formulas of Toyozawa to the yellow nP-excitons considering several corrections. This allows us to calculate the observed line widths within the same order of magnitude when compared to the experiment [10]. In Sec. II we present the main results of Toyozawa's theory. In contrast to earlier works on this topic, we perform calculations including all exciton states and no approximations as regards the phonon wave vector [15, 21]. In Sec. III A we calculate for the first time the effect of both acoustic phonons and optical phonons as well as the central-cell corrections of the $1S$-exciton state [16] on the line widths in the absorption spectrum. Furthermore, we present a detailed list of a variety of effects explaining the remaining differences between theory and experiment in Sec. III B. Finally, we give a short summary and outlook in Sec. IV.

II. THEORY

We will not present the complete theory of exciton-phonon coupling here, but only present the main results of Toyozawa's theory. Readers being interested in this topic are referred to Refs. [15, 18–20, 22].

In general, the exciton couples to two different kinds of phonons: to longitudinal acoustic phonons (LA) via deformation potential coupling [23] and to longitudinal optical phonons (LO) via the Fröhlich interaction [24]. For both interactions the interaction Hamiltonian is of

the same form in second quantization

$$H_{\mathrm{exc-ph}} = i\sum_{\boldsymbol{q}}\sum_{\nu\nu'\boldsymbol{K}}\lambda_s\left(\boldsymbol{q},\,\nu\nu'\right) \times\left(a_s\left(\boldsymbol{q}\right)-a_s^{\dagger}\left(-\boldsymbol{q}\right)\right)B_{\nu\boldsymbol{K}}^{\dagger}B_{\nu'\boldsymbol{K}-\boldsymbol{q}}. \quad (2)$$

By $a_s^{(\dagger)}\left(\boldsymbol{q}\right)$ we denote the operators annihilating (creating) a phonon in the mode $s\boldsymbol{q}$. The operators $B_{\nu\boldsymbol{K}}^{(\dagger)}$ annihilate (create) excitons with momentum $\hbar\boldsymbol{K}$ in the state $|\nu\rangle=|nlm\rangle$. Since we make use of the simple hydrogenlike model, we treat the quantum numbers n, l and m as known from atomic physics as good quantum numbers; although this is generally not the case due to the cubic symmetry of the solid [11, 13]. We will discuss this problem in Sec. III B. The coupling matrix elements are given by

$$\lambda_{\mathrm{LA}}\left(\boldsymbol{q},\,\nu\nu'\right)=f_{\mathrm{LA}}\left(q\right)\left[D_{\mathrm{e}}q_{\mathrm{e}}\left(\boldsymbol{q},\,\nu\nu'\right)-D_{\mathrm{h}}q_{\mathrm{h}}\left(\boldsymbol{q},\,\nu\nu'\right)\right] \quad (3a)$$

with

$$f_{\mathrm{LA}}\left(q\right)=\sqrt{\frac{\hbar}{2c_{\mathrm{LA}}\rho V}}q^{\frac{1}{2}} \quad (3b)$$

for LA phonons with the dispersion $\omega_{\mathrm{LA}}\left(\boldsymbol{q}\right)=c_{\mathrm{LA}}q$ including the velocity of sound c_{LA} and by

$$\lambda_{\mathrm{LO}}\left(\boldsymbol{q},\,\nu\nu'\right)=f_{\mathrm{LO}}\left(q\right)\left[q_{\mathrm{e}}\left(\boldsymbol{q},\,\nu\nu'\right)-q_{\mathrm{h}}\left(\boldsymbol{q},\,\nu\nu'\right)\right] \quad (4a)$$

with

$$f_{\mathrm{LO}}\left(q\right)=\sqrt{\frac{\hbar e^2\omega_{\mathrm{LO}}}{2V\varepsilon_0}\left(\frac{1}{\varepsilon_{\mathrm{b}}}-\frac{1}{\varepsilon_s}\right)}\frac{1}{q} \quad (4b)$$

for LO phonons with the dispersion $\omega_{\mathrm{LO}}\left(\boldsymbol{q}\right)=$ const. These matrix elements include the mass density ρ and volume V of the solid, the deformation coupling potentials $D_{\mathrm{e/h}}$ of conduction band and valence band, the dielectric constants above (ε_{b}) and below (ε_{s}) the optical resonance as well as the effective charges as defined by Toyozawa [18]:

$$q_{\mathrm{e}}\left(\boldsymbol{q},\,\nu\nu'\right) = \int\mathrm{d}\boldsymbol{r}\,\psi_{\nu}^{*}\left(\boldsymbol{r}\right)\psi_{\nu'}\left(\boldsymbol{r}\right)e^{i\frac{m_{\mathrm{h}}}{M}\boldsymbol{q}\boldsymbol{r}}, \quad (5a)$$

$$q_{\mathrm{h}}\left(\boldsymbol{q},\,\nu\nu'\right) = \int\mathrm{d}\boldsymbol{r}\,\psi_{\nu}^{*}\left(\boldsymbol{r}\right)\psi_{\nu'}\left(\boldsymbol{r}\right)e^{-i\frac{m_{\mathrm{e}}}{M}\boldsymbol{q}\boldsymbol{r}}. \quad (5b)$$

By $m_{\mathrm{e/h}}$ we denote the effective masses of electron and hole.

The interaction with phonons leads to peaks of asymmetric Loretzian shape in the absorption spectrum. The absorption coefficient depending on the frequency of light is given by [15, 18]

$$\alpha\left(\omega\right)=\sum_{\nu}\frac{\alpha_0}{\omega}\tilde{F}_{\nu}\left(\omega\right)\frac{\hbar\tilde{\Gamma}_{\nu\boldsymbol{0}}\left(\omega\right)+2\tilde{A}_{\nu}\left(\omega\right)\left[\hbar\omega-\tilde{E}_{\nu\boldsymbol{0}}\left(\omega\right)\right]}{\left[\hbar\omega-\tilde{E}_{\nu\boldsymbol{0}}\left(\omega\right)\right]^2+\left[\hbar\tilde{\Gamma}_{\nu\boldsymbol{0}}\left(\omega\right)\right]^2} \quad (6)$$

with the energy shift

$$\tilde{\Delta}_{\nu\boldsymbol{0}}\left(\omega\right)=\tilde{E}_{\nu\boldsymbol{0}}\left(\omega\right)-E_{\nu\boldsymbol{0}}=\Delta_{\nu\nu\boldsymbol{0}}\left(\omega\right)+\sum_{\nu'\neq\nu}\frac{\left|\Delta_{\nu\nu'\boldsymbol{0}}\left(\omega\right)\right|^2-\left|\Gamma_{\nu\nu'\boldsymbol{0}}\left(\omega\right)\right|^2}{E_{\nu\boldsymbol{0}}-E_{\nu'\boldsymbol{0}}}, \quad (7)$$

the line broadening

$$\tilde{\Gamma}_{\nu\boldsymbol{0}}\left(\omega\right)=\Gamma_{\nu\nu\boldsymbol{0}}\left(\omega\right)+\sum_{\nu'\neq\nu}2\,\mathrm{Re}\left(\frac{\Delta_{\nu\nu'\boldsymbol{0}}\left(\omega\right)\Gamma_{\nu'\nu\boldsymbol{0}}\left(\omega\right)}{E_{\nu\boldsymbol{0}}-E_{\nu'\boldsymbol{0}}}\right), \quad (8)$$

the scaling of the constant amplitude α_0

$$\begin{aligned}\tilde{F}_{\nu}\left(\omega\right) &= \left|M_{\nu g}\right|^2+\sum_{\nu'\neq\nu}2\,\mathrm{Re}\left(\frac{M_{\nu g}^{*}\Delta_{\nu\nu'\boldsymbol{0}}\left(\omega\right)M_{\nu' g}}{E_{\nu\boldsymbol{0}}-E_{\nu'\boldsymbol{0}}}\right)\\ &+\sum_{\nu'\neq\nu}\sum_{\nu''\neq\nu}2\,\mathrm{Re}\left(\frac{M_{\nu g}^{*}\left(\Delta_{\nu\nu''\boldsymbol{0}}\left(\omega\right)\Delta_{\nu''\nu'\boldsymbol{0}}\left(\omega\right)-\Gamma_{\nu\nu''\boldsymbol{0}}\left(\omega\right)\Gamma_{\nu''\nu'\boldsymbol{0}}\left(\omega\right)\right)M_{\nu' g}}{\left(E_{\nu\boldsymbol{0}}-E_{\nu'\boldsymbol{0}}\right)\left(E_{\nu\boldsymbol{0}}-E_{\nu''\boldsymbol{0}}\right)}\right)\\ &+\sum_{\nu'\neq\nu}\sum_{\nu''\neq\nu}\mathrm{Re}\left(\frac{M_{\nu' g}^{*}\left(\Delta_{\nu'\nu\boldsymbol{0}}\left(\omega\right)\Delta_{\nu\nu''\boldsymbol{0}}\left(\omega\right)-\Gamma_{\nu'\nu\boldsymbol{0}}\left(\omega\right)\Gamma_{\nu\nu''\boldsymbol{0}}\left(\omega\right)\right)M_{\nu'' g}}{\left(E_{\nu\boldsymbol{0}}-E_{\nu'\boldsymbol{0}}\right)\left(E_{\nu\boldsymbol{0}}-E_{\nu''\boldsymbol{0}}\right)}\right), \end{aligned} \quad (9)$$

and the asymmetry $\tilde{A}_\nu(\omega)$, which can be calculated from

$$\begin{aligned}\tilde{A}_\nu(\omega)\,\tilde{F}_\nu(\omega) &= \sum_{\nu'\neq\nu}\mathrm{Re}\left(\frac{M^*_{\nu g}\Gamma_{\nu\nu'\mathbf{0}}(\omega)\,M_{\nu' g}}{E_{\nu\mathbf{0}}-E_{\nu'\mathbf{0}}}\right)\\ &+\sum_{\nu'\neq\nu}\sum_{\nu''\neq\nu}2\,\mathrm{Re}\left(\frac{M^*_{\nu g}\left(\Delta_{\nu\nu''\mathbf{0}}(\omega)\,\Gamma_{\nu''\nu'\mathbf{0}}(\omega)+\Gamma_{\nu\nu''\mathbf{0}}(\omega)\,\Delta_{\nu''\nu'\mathbf{0}}(\omega)\right)M_{\nu' g}}{(E_{\nu\mathbf{0}}-E_{\nu'\mathbf{0}})\,(E_{\nu\mathbf{0}}-E_{\nu''\mathbf{0}})}\right)\\ &+\sum_{\nu'\neq\nu}\sum_{\nu''\neq\nu}\mathrm{Re}\left(\frac{M^*_{\nu' g}\left(\Delta_{\nu'\nu\mathbf{0}}(\omega)\,\Gamma_{\nu\nu''\mathbf{0}}(\omega)-\Gamma_{\nu'\nu\mathbf{0}}(\omega)\,\Delta_{\nu\nu''\mathbf{0}}(\omega)\right)M_{\nu'' g}}{(E_{\nu\mathbf{0}}-E_{\nu'\mathbf{0}})\,(E_{\nu\mathbf{0}}-E_{\nu''\mathbf{0}})}\right).\end{aligned}\tag{10}$$

The quantity $M_{\nu g}$ denotes the transition matrix element between the ground state $|0\rangle$ of the solid and the exciton state $|\nu\rangle$ with $\boldsymbol{K}=0$ due to the electron-photon interaction. In cuprous oxide the transition is parity-forbidden, which results in [8]

$$M_{\nu g}=c\,\frac{n^2-1}{n^5}\delta_{l,1}\delta_{m,0}.\tag{11}$$

Since in both equations (9) and (10) $M_{\nu g}$ appears quadratically, the asymmetry $\tilde{A}_\nu(\omega)$ will be independent of the proportionality constant c. The main difficulty in the implementation of the formulas given above is the calculation of the quantities [15, 18]

$$\begin{aligned}\Gamma_{\nu_2\nu_1\mathbf{0}}(\omega) &= \sum_{s\boldsymbol{q}}\sum_{\nu_3}\frac{\pi}{\hbar}\lambda^*_s(\boldsymbol{q},\,\nu_3\nu_2)\,\lambda_s(\boldsymbol{q},\,\nu_3\nu_1)\\ &\times\left[(n_s(\boldsymbol{q},\,T)+1)\,\delta\left(E_{\nu_3\boldsymbol{q}}+\hbar\omega_s(\boldsymbol{q})-\hbar\omega\right)+n_s(\boldsymbol{q},\,T)\,\delta\left(E_{\nu_3\boldsymbol{q}}-\hbar\omega_s(\boldsymbol{q})-\hbar\omega\right)\right],\end{aligned}\tag{12}$$

and

$$\begin{aligned}\Delta_{\nu_2\nu_1\mathbf{0}}(\omega) &= \sum_{s\boldsymbol{q}}\sum_{\nu_3}\lambda^*_s(\boldsymbol{q},\,\nu_3\nu_2)\,\lambda_s(\boldsymbol{q},\,\nu_3\nu_1)\\ &\times\left[(n_s(\boldsymbol{q},\,T)+1)\,\mathcal{P}\left(\frac{1}{\hbar\omega-E_{\nu_3\boldsymbol{q}}-\hbar\omega_s(\boldsymbol{q})}\right)+n_s(\boldsymbol{q},\,T)\,\mathcal{P}\left(\frac{1}{\hbar\omega-E_{\nu_3\boldsymbol{q}}+\hbar\omega_s(\boldsymbol{q})}\right)\right].\end{aligned}\tag{13}$$

The symbol $\mathcal{P}$ denotes the principal value. We can write

$$\mathcal{P}\left(\frac{1}{x}\right)=\mathcal{P}\int\mathrm{d}E\,\frac{1}{E}\delta(E-x)\lim_{\epsilon\to0^+}\left(\int_{-\infty}^{-\epsilon}\mathrm{d}E\,\frac{1}{E}\delta(E-x)+\int_{\epsilon}^{\infty}\mathrm{d}E\,\frac{1}{E}\delta(E-x)\right).\tag{14}$$

The average thermal occupation of phononic states at a temperature T is given by [22]

$$n_s(\boldsymbol{q},\,T)=\frac{1}{e^{\hbar\omega_s(\boldsymbol{q})/k_\mathrm{B}T}-1}.\tag{15}$$

The evaluation of $\Gamma_{\nu_2\nu_1\mathbf{0}}(\omega)$ and $\Delta_{\nu_2\nu_1\mathbf{0}}(\omega)$ as well as their application to Cu_2O are presented in the Appendix.

III. RESULTS AND DISCUSSION

A. Contributions to the line widths

In the following we will discuss the different contributions to the line widths $\tilde{\Gamma}_{\nu\mathbf{0}}(\omega)$ in Eq. (8) for Cu_2O at the very low temperature of $T=1.2\,\mathrm{K}$ [10]. The relevant material parameters are listed in Table I. Although the unit cell of Cu_2O comprises 6 atoms, which amounts in 15 optical phonon modes, there are only two LO-phonon modes with Γ_4^--symmetry contributing to the Fröhlich interaction [16].

For our discussion we will especially consider the line parameters of the $2P$-exciton since it has always been wondered which effects lead to the large broadening of this line [18, 28–30]. We discuss the contributions to these parameters in several steps.

Step 1: We start with the most simple case, in which we neglect the optical phonons, set the frequency ω to $E_{\nu\mathbf{0}}/\hbar$ and neglect the so-called intraband-contributions [18], i.e., we only include those parts of

TABLE I: Material parameters of Cu_2O used in our calculations. m_0 denotes the free electron mass. All values are taken from Ref. [25] unless otherwise stated.

Parameter	Value
Lattice constant	$a = 4.27 \times 10^{-10}\,\mathrm{m}$
Mass density	$\rho = 6.09\,\frac{\mathrm{g}}{\mathrm{cm}^3}$
Band gap energy	$E_\mathrm{g} = 2.17\,\mathrm{eV}$
Effective masses [26]	$m_\mathrm{e} = 0.99 m_0$
	$m_\mathrm{h} = 0.58 m_0$
Dielectric constants	$\varepsilon_{\mathrm{s}1} = 7.5$, $\varepsilon_{\mathrm{b}1} = 7.11$
	$\varepsilon_{\mathrm{s}2} = 7.11$, $\varepsilon_{\mathrm{b}2} = 6.46$
Sound wave velocity	$c_\mathrm{LA} = 4.5405 \times 10^3\,\frac{\mathrm{m}}{\mathrm{s}}$
Energy of Γ_4^--LO phonons [16]	$\hbar\omega_{\mathrm{LO},1} = 18.7\,\mathrm{meV}$
	$\hbar\omega_{\mathrm{LO},2} = 87\,\mathrm{meV}$
Deformation potentials [27]	$D_\mathrm{e} = 2.4\,\mathrm{eV}$
	$D_\mathrm{h} = 2.2\,\mathrm{eV}$
Rydberg energy [11]	$R_\mathrm{exc} = 86\,\mathrm{meV}$

Eqs. (7)-(10), which do not contain sums over ν'. The approximation of setting $\omega \approx E_{\nu\mathbf{0}}/\hbar$ is justified since $\tilde{\Gamma}_{\nu\mathbf{0}}(\omega)$ is a slowly varying function with ω [15, 28]. The formula (12) includes a sum over all excitonic states. In order to calculate the quantity $\Gamma_{\nu_2\nu_1\mathbf{0}}(\omega)$ within reasonable time, we have to restrict the infinite sum to a finite one via

$$\sum_{\nu_3} \to \sum_{n_3=1}^{n_\mathrm{max}} \sum_{l_3=0}^{n_3-1} \sum_{m_3=-l_3}^{l_3} \tag{16}$$

with $n_\mathrm{max} \leq 7$. As it has also been done by Toyozawa [18], one may at first include only states having the same principal quantum number as the one considered. This means for the $2P$-exciton that the sum reads

$$\sum_{\nu_3} \to \sum_{n_3=2}^{2} \sum_{l_3=0}^{1} \sum_{m_3=-l_3}^{l_3} . \tag{17}$$

This yields very small values for the line width and the energy shift

$$\tilde{\Gamma}_{210\,\mathbf{0}}(E_{210\,\mathbf{0}}/\hbar) \approx 1.70 \times 10^{-9}\,\mathrm{eV}, \tag{18a}$$

$$\tilde{\Delta}_{210\,\mathbf{0}}(E_{210\,\mathbf{0}}/\hbar) \approx -9.72 \times 10^{-6}\,\mathrm{eV}. \tag{18b}$$

Step 2: An obviously better approach is to evaluate the complete sum (16) with different n_max and extrapolate the values obtained for $\tilde{\Gamma}_{210\,\mathbf{0}}$ and $\tilde{\Delta}_{210\,\mathbf{0}}$ to the final value for $n_\mathrm{max} \to \infty$. To this aim we fit a function of the form $f(n_\mathrm{max}) = a/n_\mathrm{max}^2 + b$ to our values. We depict this procedure in Fig. 1. This approach yields

$$\tilde{\Gamma}_{210\,\mathbf{0}}(E_{210\,\mathbf{0}}/\hbar) \approx 9.87 \times 10^{-7}\,\mathrm{eV}, \tag{19a}$$

$$\tilde{\Delta}_{210\,\mathbf{0}}(E_{210\,\mathbf{0}}/\hbar) \approx -2.32 \times 10^{-5}\,\mathrm{eV}. \tag{19b}$$

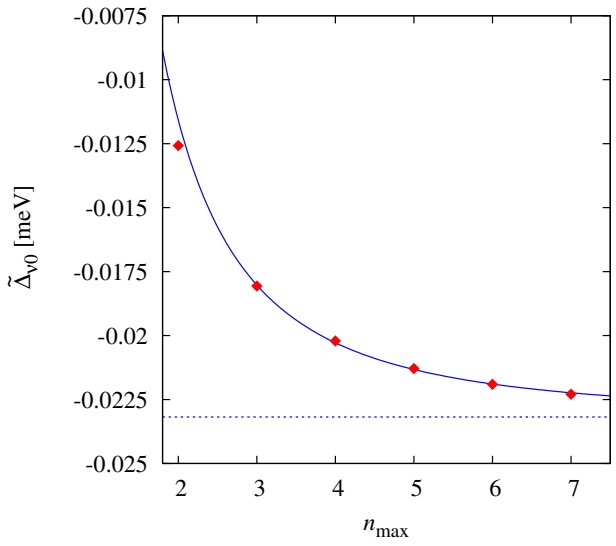

FIG. 1: (Color online) In order to evaluate the quantities $\Gamma_{\nu_2\nu_1\mathbf{0}}(\omega)$ and $\Delta_{\nu_2\nu_1\mathbf{0}}(\omega)$, one has to cut the infinite sums over ν in the formulas at a finite value n_max of the principal quantum number n (cf. Eq. (16)). Here we show the values obtained for $\tilde{\Delta}_{210\,\mathbf{0}}$ in dependence on n_max for *Step 2*. The final value $\tilde{\Delta}_{210\,\mathbf{0}} = -2.32 \times 10^{-5}\,\mathrm{eV}$ (dashed line) is then calculated from an extrapolation. We used $f(n_\mathrm{max}) = a/n_\mathrm{max}^2 + b$ as a fitting function for $n_\mathrm{max} \geq 3$ (solid line).

This already shows that the $1S$-exciton state has a large influence on the line width of the $2P$-state.

Step 3: At very low temperatures only few LA phonons are thermally excited. We therefore expect the optical phonons to increase the line width considerably; especially since the energy of one of these phonons ($\hbar\omega_{\mathrm{LO},1} = 18.7\,\mathrm{meV}$) is of the same magnitude as the energetic difference between two exciton states ($E_{210\,\mathbf{0}} - E_{410\,\mathbf{0}} \approx 17.25\,\mathrm{meV}$). Including optical phonons, we obtain

$$\tilde{\Gamma}_{210\,\mathbf{0}}(E_{210\,\mathbf{0}}/\hbar) \approx 3.45 \times 10^{-5}\,\mathrm{eV}, \tag{20a}$$

$$\tilde{\Delta}_{210\,\mathbf{0}}(E_{210\,\mathbf{0}}/\hbar) \approx -8.39 \times 10^{-3}\,\mathrm{eV}. \tag{20b}$$

Step 4: Up to now we have assumed that the line width $\tilde{\Gamma}_{210\,\mathbf{0}}(\omega)$ is a slowly varying function of the frequency of light. For this reason we have set $\omega \approx E_{\nu\mathbf{0}}/\hbar$. In the literature it has been discussed that it is necessary to account for the frequency dependence in order to describe the asymmetry of the lines correctly [28]. On the other hand, Toyozawa already stated in Ref. [15] that the line shape would not be of asymmetric Lorentzian shape if $\tilde{\Gamma}_{210\,\mathbf{0}}(\omega)$ varied strongly with ω. We see that the energy shift $\tilde{\Delta}_{210\,\mathbf{0}}$ is several meV large. Since the absorption peak is centered around $\tilde{E}_{\nu\mathbf{0}}(\omega)$, we evaluate the line

parameters within the range $\omega_{\min} \leq \omega \leq \omega_{\max}$ with

$$\hbar\omega_{\min} = E_{210\,\mathbf{0}} - 2\left|\tilde{\Delta}_{210\,\mathbf{0}}\left(E_{210\,\mathbf{0}}/\hbar\right)\right| \tag{21}$$

and

$$\hbar\omega_{\max} = E_{210\,\mathbf{0}} \tag{22}$$

to determine their frequency dependence. It is found that $\tilde{\Gamma}_{210\,\mathbf{0}}(\omega)$ increases slowly with ω while $\tilde{\Delta}_{210\,\mathbf{0}}(\omega)$ decreases strongly :

$$\tilde{\Gamma}_{210\,\mathbf{0}}(\omega_{\min}) \approx 3.30 \times 10^{-5}\,\mathrm{eV}, \tag{23a}$$
$$\tilde{\Gamma}_{210\,\mathbf{0}}(\omega_{\max}) \approx 3.45 \times 10^{-5}\,\mathrm{eV}, \tag{23b}$$

$$\tilde{\Delta}_{210\,\mathbf{0}}(\omega_{\min}) \approx -6.97 \times 10^{-3}\,\mathrm{eV}, \tag{23c}$$
$$\tilde{\Delta}_{210\,\mathbf{0}}(\omega_{\max}) \approx -8.39 \times 10^{-3}\,\mathrm{eV}. \tag{23d}$$

The effect on the line width may be more important in external fields, which would mix different excitonic states [18, 31].

Step 5: An important effect concerns the $1S$-exciton of the yellow series of Cu_2O. The mean distance between electron and hole is so small that this exciton can hardly be treated as a Wannier exciton. The corrections that have to be made due to this small distance are known as the central-cell corrections. They lead to a higher mass of the $1S$-exciton of $\tilde{M} \approx 3m_0$ and to a smaller excitonic Bohr radius of $\tilde{a}_{\mathrm{exc}} \approx 0.53\,\mathrm{nm}$ [16]. These corrections are now included in the excitonic wave function ψ_{100} and in the excitonic energies

$$E_{100\,\boldsymbol{K}} = E_{\mathrm{gap}} - \frac{\tilde{R}_{\mathrm{exc}}}{n^2} + \frac{\hbar^2\boldsymbol{K}^2}{2\tilde{M}}. \tag{24}$$

The binding energy $\tilde{R}_{\mathrm{exc}} \approx 153\,\mathrm{meV}$ of the $1S$-exciton differs much from the excitonic Rydberg constant of the rest of the yellow exciton series. The central-cell corrections have a significant influence on the line width and increase it by a factor of about 17 to

$$\tilde{\Gamma}_{210\,\mathbf{0}}(\omega_{\min}) \approx 6.12 \times 10^{-4}\,\mathrm{eV}, \tag{25a}$$
$$\tilde{\Gamma}_{210\,\mathbf{0}}(\omega_{\max}) \approx 5.53 \times 10^{-4}\,\mathrm{eV}, \tag{25b}$$

$$\tilde{\Delta}_{210\,\mathbf{0}}(\omega_{\min}) \approx -6.98 \times 10^{-3}\,\mathrm{eV}, \tag{25c}$$
$$\tilde{\Delta}_{210\,\mathbf{0}}(\omega_{\max}) \approx -8.18 \times 10^{-3}\,\mathrm{eV}. \tag{25d}$$

Step 6: We now investigate the influence of intraband scattering. Therefore, we also consider the sums of the form $\sum_{\nu'\neq\nu}$ in Eqs. (7)-(10), where we also cut these sums at the same value of $n_{\max}$. In contrast to the expectation of Toyozawa [15], the effect of this type of scattering on the line width is quite small. We obtain

$$\tilde{\Gamma}_{210\,\mathbf{0}}(\omega_{\min}) \approx 4.04 \times 10^{-4}\,\mathrm{eV}, \tag{26a}$$
$$\tilde{\Gamma}_{210\,\mathbf{0}}(\omega_{\max}) \approx 4.94 \times 10^{-4}\,\mathrm{eV}, \tag{26b}$$

$$\tilde{\Delta}_{210\,\mathbf{0}}(\omega_{\min}) \approx -7.14 \times 10^{-3}\,\mathrm{eV}, \tag{26c}$$
$$\tilde{\Delta}_{210\,\mathbf{0}}(\omega_{\max}) \approx -8.57 \times 10^{-3}\,\mathrm{eV}. \tag{26d}$$

Nevertheless, the asymmetry of the lines can be explained only by intraband scattering. The value of

$$\tilde{A}_{210}(\omega_{\min}) \approx -3.67 \times 10^{-2}, \tag{26e}$$
$$\tilde{A}_{210}(\omega_{\max}) \approx -3.69 \times 10^{-2}, \tag{26f}$$

is, however, very small in comparison with the large asymmetry of the lines observed in [10]. We will discuss this discrepancy in Sec. III B.

Step 7: In the literature a large asymmetry has also been assigned to a coupling of the bound exciton states to the continuum states [28, 32–34], whose energies are given by

$$E_{\boldsymbol{k}\,\boldsymbol{K}} = E_{\mathrm{gap}} + \frac{\hbar^2\boldsymbol{k}^2}{2\mu} + \frac{\hbar^2\boldsymbol{K}^2}{2M} \tag{27}$$

in analogy to the hydrogen atom. However, an effect of the continuum states can be excluded via a simple calculation: For the average occupation of the phonon modes one obtains $n_{\mathrm{LO},1}(\boldsymbol{q}, T) = 0$ for $T \lesssim 25\,\mathrm{K}$ and $n_{\mathrm{LO},2}(\boldsymbol{q}, T) = 0$ for $T \lesssim 100\,\mathrm{K}$, i.e., only scattering processes with the emission of phonons can take place at $T = 1.2\,\mathrm{K}$. Furthermore, the emission process can only take place if the arguments of the δ-functions in Eqs. (12) and (13) are positive. This means for acoustic phonons

$$\frac{\hbar^2\boldsymbol{k}^2}{2\mu} < \frac{1}{2}Mc_{\mathrm{LA}}^2 - \frac{R_{\mathrm{exc}}}{n^2} \tag{28a}$$

and for optical phonons

$$\frac{\hbar^2\boldsymbol{k}^2}{2\mu} < -\hbar\omega_{\mathrm{LO}} - \frac{R_{\mathrm{exc}}}{n^2}. \tag{28b}$$

Therefore, only LA phonons play a role and only for the line shapes of excitons with $n > 32$. A contribution of the continuum states is therefore impossible.

The final results including all of the corrections discussed above are listed in Table II. We also list the experimental line widths, which have been obtained by fitting Lorentzians or Elliotts formula to the experimental absorption spectrum (cf. Fig. 2). It can be seen that we obtain the correct behavior of the line parameters with increasing principal quantum number: The line widths decrease with increasing quantum number.

In Fig. 2 we compare the predicted line shapes with the measured ones. It is obvious that our calculation cannot reproduce quantitatively the large asymmetry. However, the line widths differ only by a factor of ~ 3.5 or even ~ 1.3, which means that they are of the same order of magnitude. The observable difference in the position of the lines can be explained on the one hand by small inaccuracies of the material constants used, on the other hand in terms of the complex valence band structure of Cu_2O. These facts and further possible reasons for deviations from the experimental spectrum will be discussed in Sec. III B.

A quantitative comparison of the calculated line widths with the results of previous works is not possible. In

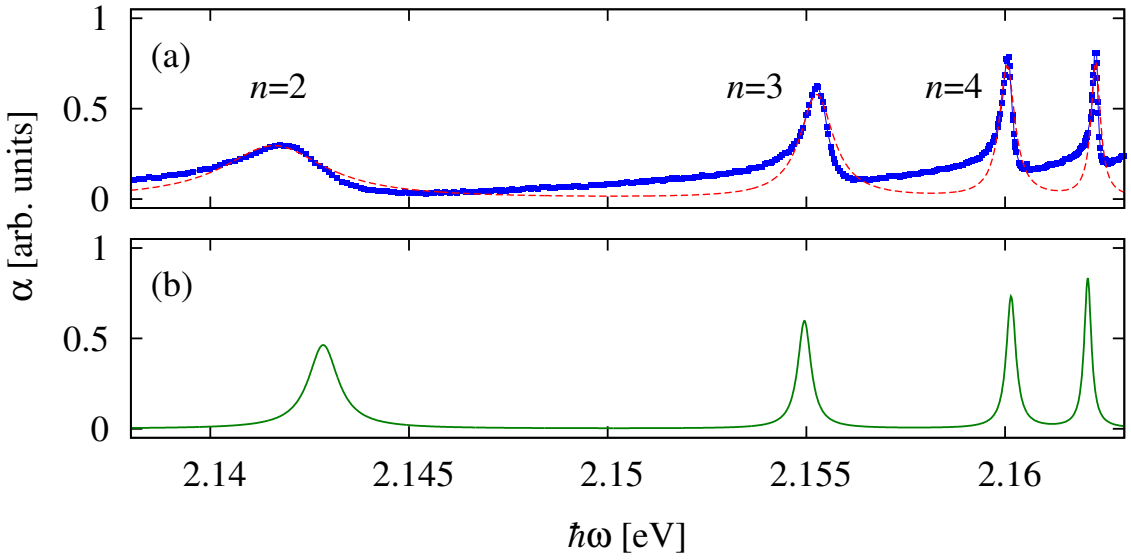

FIG. 2: (Color online) Comparison of (a) the experimental spectrum [10] with (b) the calculated line shapes using Eq. (6) and the values listed in Table II. Since we do not know the proportionality constant c in Eq. (11), we chose arbitrary values for the amplitudes $\tilde{F}_\nu(\omega)$. We shifted the experimental values by an amount of -6 meV for a better comparison. The experimental values have been fitted by Lorentzians to obtain the experimental line widths (red dashed line).

TABLE II: The final values for the line widths $\tilde{\Gamma}_{\nu\mathbf{0}}$, the energy shifts $\tilde{\Delta}_{\nu\mathbf{0}}$ including all of the corrections discussed in Sec. III A. The values are given at $\hbar\omega = E_{n10\,\mathbf{0}} - \tilde{\Delta}_{n10\,\mathbf{0}}(E_{n10\,\mathbf{0}}/\hbar)$ (cf. *Step 4* of Sec. III A). In the last column the experimental line widths are listed [10].

ν	$\tilde{\Gamma}_{\nu\mathbf{0}}$ [meV]	$\tilde{\Delta}_{\nu\mathbf{0}}$ [meV]	$\tilde{\Gamma}_{\nu\mathbf{0}}$(exp) [meV]
210	0.453	−7.737	1.581
310	0.201	−7.574	0.511
410	0.144	−6.551	0.237
510	0.108	−6.560	0.142

Ref. [18] it is reported that the calculated line width of the $2P$-exciton is several times smaller than the experimentally observed one but no value is given. In Ref. [21] the calculated line widths are several times larger than the experimental ones indicating the inappropriateness of the many approximations in that publication.

B. Further discussion

In the above calculation we made some assumptions, which are discussed in the following. We also discuss possible causes for a further broadening of the lines, which may be difficult to be considered in theory.

We have assumed that the dispersion of LA phonons is linear according to $\omega_{\mathrm{LA}} = c_{\mathrm{LA}} q$ and that the dispersion of LO phonons is constant. If we perform the q-integration according to Eq. (A.1b) only up to a value of $q_{\max} < q_{\mathrm{D}}$, our results do not change for $\frac{1}{2}q_{\mathrm{D}} < q_{\max} < q_{\mathrm{D}}$, i.e., we can always set the upper boundary of the integral to $\frac{1}{2}q_{\mathrm{D}}$. Since the assumption of the LA dispersion relation to be linear in q holds for $q < \frac{1}{2}q_{\mathrm{D}}$ [35–38], its usage is retroactively justified. Furthermore, the change of the energy of the LO phonons within this limit is very small [39].

We have treated l and m as good quantum numbers in the above calculations. This is in general not the case due to the cubic symmetry of the crystal. Nevertheless, since $\mathrm{O_h}$ is the point group with the highest symmetry, it may be justified to treat l approximatively as a good quantum number [11, 13]. However, one would still have to calculate the correct linear combinations of states with different m quantum number, which then transform according to the irreducible representations of the cubic group $\mathrm{O_h}$ [13]. This has not been done since we expect no effect from this rearrangement of states.

The asymmetry of the lines calculated in *Step 6* are considerably smaller than the experimental values. The large asymmetries can be explained in terms of Fano resonances and phonon replicas. Phonon replicas describe, in particular for luminescence, the scattering of a polariton from the exciton-like branch of its dispersion relation to the photon-like branch with the simultaneous emission of LO phonons, or more simply the decay of an exciton with the emission of one photon and LO phonons. In luminescence spectra the line shape then shows a square-root-like energy dependence due to the exciton density of states. While LO-phonon replicas appear on the low-energy side in luminescence spectra, they can also appear on the high-energy side in absorption spectra [40]. In the

case of Cu_2O the Γ_3^- LO phonon assists the $1S$ exciton formation and causes the square-root-like frequency dependence of the absorption coefficient, on which then absorption of the other exciton resonances is superimposed (see, e.g., Refs. [21, 41, 42]). Since the transition amplitudes interfere destructively or constructively on the lower or higher energy side of the resonance with the continuum of the Γ_3^- LO phonon, one obtains asymmetric line shapes of the exciton resonances in accordance with the theory of Fano resonances [43]. Since the formulas of Sec. II do not account for the phononic background, we could not determine correct asymmetries of the lines. Note that the phononic background has been subtracted from the results of Ref. [10]; an absorption spectrum including it can be found, e.g., in Ref. [44]. For further information on this topic, see also Refs. [40, 45] and further references therein.

The Rydberg energies R_{exc} of excitonic spectra are generally obtained from fits to experimental results. Therefore, the value of R_{exc} for the yellow series of Cu_2O varies between 86 meV [11] and 97.2 meV [46] in the literature. The same argument holds for the band gap energy E_{gap}. One reason for the deviations in the line positions in Fig. 2 is thus the uncertainity in these constants.

We have also assumed that the simple band model holds. Indeed, the results in [10] show that this approximation is reasonable; but one could also include the complete valence band structure in the theory [13, 17]. This makes an investigation of line widths almost impossible since the energies $E_{\nu \boldsymbol{K}}$ have to be determined first of all, and a separation of relative motion and the motion of the center of mass is not possible [47, 48]. The calculations in Ref. [47] on the line widths of the $1S$-exciton states of different semiconductors already show the main problems if one would have to extend the theory to principal quantum numbers of $n \geq 2$. On the other hand, an inclusion of the complete valence band structure results in a coupling of the yellow and green exciton series, especially to the green $1S$-exciton state [17]. Since we found out that the yellow $1S$-exciton state has a significant influence on the line width of the $2P$-exciton state, we expect that the coupling to the green $1S$-exciton state will lead to a further broadening of this line. The coupling to the (energetically higher located) green series may also be a reason for the large degree of asymmetry of the lines.

The complex valence band structure is sometimes treated in a simple approach in terms of quantum defects [10, 11]. However, the results of Ref. [11] show that this approach works well only at high quantum numbers ($n \geq 7$). Therefore, we did not consider quantum defects in our calculations.

The complex valence band structure also facilitates a coupling of excitons to TA phonons [22, 47, 49]. However, the effect of TA phonons is reported to be half as large as the effect of LA phonons [35, 50], which is already very small in our case. The coupling to TA phonons may be more important if external strains are applied to the crystal [51].

Impurities, especially point defects, in the crystal can lead to a broadening of exciton line widths [52]. The effect of an increase in the defect concentration has, according to Toyozawa [18], the same effect as a raising of the temperature. However, it has been discussed in the literature that a large concentration of impurities will lead to a more Gaussian or Voigt line shape [47, 53, 54]. This cannot be seen in the line spectrum measured in Ref. [10], for which reason we have to assume that the concentration of defects is low. Certainly, one could also estimate the concentration of defects experimentally by an extrapolation of the line width to $T \to 0\,\mathrm{K}$ [55]. Furthermore, the effect of a movement of defects being caused by phonons is said to be negligible [47].

The Fröhlich coupling constant is defined as [22]

$$\alpha^{\mathrm{F}} = \frac{e^2}{8\pi\varepsilon_0\hbar\omega_{\mathrm{LO}}} \left(\frac{2M\omega_{\mathrm{LO}}}{\hbar}\right)^{\frac{1}{2}} \left(\frac{1}{\varepsilon_{\mathrm{b}}} - \frac{1}{\varepsilon_s}\right) \quad (29)$$

For Cu_2O we obtain $\alpha_1^{\mathrm{F}} \approx 0.24$ and $\alpha_2^{\mathrm{F}} \approx 0.20$. Since these values are clearly smaller than 1, we can neglect polaron corrections to the energy and the mass of the excitons [22, 31].

In the unit cell of Cu_2O there are always four copper atoms arranged in tetragonal symmetry [56], but only in every second tetragon an oxygen atom is located at its center. Since the oxygen atoms are very small, there is a chance that there are sometimes more than two oxygen atom in one unit cell. The excess atoms will then occupy the free positions in the lattice and act as acceptors. This results in small charges and in small internal electric fields, which will influence the exciton and lead to a line broadening. However, it is hard to account for these fields in theory.

The coupling between excitons and phonons is linear, i.e., there is always only one phonon being involved in a scattering process. In the literature, multi-phonon processes are said to be important in connection with piezoelectric coupling [28]. Sometimes, they are even said to be negligible [53]. Since piezoelectric coupling is symmetry-forbidden in Cu_2O, we do not consider multi-phonon processes.

In general, there are no excitons in crystals but polaritons due to the coupling to light [8]. In other materials than Cu_2O the excitonic $1S$-ground state is often dipole allowed. The resulting large polariton coupling mainly changes the contribution of LA phonons to the line widths but the contribution of the LO phonons only weakly (see Ref. [31] and further references therein). Since the LA-phononic contribution is small for Cu_2O, we expect that the polariton effect will not change our results significantly, so that it can even be neglected [35].

We have shown that the central-cell corrections have a major influence on the line width of the $2P$-exciton state. Besides the central-cell corrections, which lead to an increase in the mass of the $1S$-exciton, there exists also a $\boldsymbol{K}$-dependent exchange interaction, which results in a $\boldsymbol{K}$-dependent effective mass $\tilde{M}(\boldsymbol{K})$ of this exciton [57].

We expect the influence of the $\boldsymbol{K}$-dependency of the mass $\tilde{M}$ to be small for the following reason: We have proven that the effect of interband coupling on the line width is unimportant. For this reason the main contribution to the line widths comes from the region with $\boldsymbol{K} \approx \boldsymbol{0}$ and it is sufficient to take the value $\tilde{M}(\boldsymbol{0})$ (cf. the illustrations of intraband and interband scattering in Ref. [8]).

IV. SUMMARY AND OUTLOOK

We have calculated the main parameters describing the shape of the excitonic absorption lines for the yellow exciton series of Cu_2O and compared our results to the experimentally observed lines of Ref. [10]. Especially the calculated line width for yellow $2P$-exciton lies within the same order of magnitude as the experimental one and differs only by a factor of ~ 3.5, which is a significant improvement on the result of Ref. [15]. Furthermore, we have discussed possible reasons for the large broadening and the large asymmetry of the lines. Of course, some of these special properties of Cu_2O could eventually be included in theory, but only with huge effort.

Recently, it has been shown that the yellow excitonic line spectrum of Cu_2O in an external magnetic field shows GUE statistics [12]. This line statistics has been explained in terms of the exciton-phonon coupling in the crystal. Therefore, it will be worthwhile to extend our calculations by including a magnetic field in order to prove the GUE statistics theoretically.

Acknowledgments

We thank Ch. Uihlein and D. Fröhlich for helpful discussions.

Appendix: Evaluation of $\Gamma_{\nu_2\nu_1\boldsymbol{0}}(\omega)$ and $\Delta_{\nu_2\nu_1\boldsymbol{0}}(\omega)$

We now present the evaluation of Eqs. (12) and (13) as well as their application to Cu_2O.

Due to periodic boundary conditions, the values of the phononic wave vector $\boldsymbol{q}$ are generally discrete [22]. If we apply the continuum approximation, in which the number of atoms N of the solid goes to infinity and the lattice constant a_{lat} between the atoms goes to zero while the ratio $Na_{\mathrm{lat}}^3 = V$ is kept constant, we can treat $\boldsymbol{q}$ as a continuous quantity and replace the corresponding sums by integrals:

$$\sum_{\boldsymbol{q}} \to \frac{V}{(2\pi)^3} \int \mathrm{d}\boldsymbol{q} \tag{A.1a}$$

with

$$\int \mathrm{d}\boldsymbol{q} = \int_0^{q_{\mathrm{D}}} \mathrm{d}q\, q^2 \int_0^{\pi} \mathrm{d}q_\vartheta\, \sin q_\vartheta \int_0^{2\pi} \mathrm{d}q_\varphi. \tag{A.1b}$$

The upper boundary q_{D} of the q-integral is given by the boundary of the first Brillouin zone (BZ) and can be calculated from the Debye model [22]. In order to evaluate the integral over $\boldsymbol{q}$, the dependence of the effective charges on the angles q_ϑ and q_φ has to be determined. To this end we substitute the variable $\boldsymbol{r}$ in the integrals of Eqs. (5a) and (5b) by $\boldsymbol{u} = \boldsymbol{A}^{\mathrm{T}}\boldsymbol{r}$ with a rotation matrix $\boldsymbol{A}$, for which $\boldsymbol{A}^{\mathrm{T}}\boldsymbol{q} = q\hat{\boldsymbol{e}}_z$ holds. By $\hat{\boldsymbol{e}}_z$ we denote the unit vector in z-direction. If we denote by $\boldsymbol{R}_{\hat{\boldsymbol{n}}\varphi}$ the rotation matrix describing the rotation about an axis $\hat{\boldsymbol{n}}$ by an angle φ, we can express $\boldsymbol{A}$ as

$$\boldsymbol{A} = \boldsymbol{R}_{\hat{\boldsymbol{e}}_z(-q_\alpha)}\boldsymbol{R}_{\hat{\boldsymbol{e}}_y(-q_\vartheta)}\boldsymbol{R}_{\hat{\boldsymbol{e}}_z(-q_\varphi)} \tag{A.2}$$

with an arbitrary angle q_α. The hydrogen-like wave functions ψ_ν of the exciton read

$$\psi_\nu(\boldsymbol{r}) = R_{nl}(r)Y_{lm}(\vartheta, \varphi) \tag{A.3}$$

with the spherical harmonics $Y_{lm}(\vartheta, \varphi)$. For the radial part $R_{nl}(r)$ we take the well-known functions of the hydrogen atom [58], but replace the Bohr radius a_0 by the excitonic Bohr radius a_{exc}, which is given by [22]

$$a_{\mathrm{exc}} = a_0 \frac{\mathrm{Ry}}{\varepsilon_{\mathrm{s1}} R_{\mathrm{exc}}} \approx 1.116\,\mathrm{nm}, \tag{A.4}$$

with the Rydberg energy Ry and the dielectric constant $\varepsilon_{\mathrm{s1}}$, which is given together with all other material parameters of Cu_2O in Table I.

After the substitution, we make use of the special properties of the spherical harmonics under rotations [59]:

$$\begin{aligned}
\psi_\nu(\boldsymbol{A}\boldsymbol{u}) &= e^{-\frac{i}{\hbar}q_\alpha\hat{\boldsymbol{e}}_z\boldsymbol{L}}e^{-\frac{i}{\hbar}q_\vartheta\hat{\boldsymbol{e}}_y\boldsymbol{L}}e^{-\frac{i}{\hbar}q_\varphi\hat{\boldsymbol{e}}_z\boldsymbol{L}}\psi_\nu(\boldsymbol{u}) \\
&= \mathcal{D}(q_\alpha, q_\vartheta, q_\varphi)\,\psi_\nu(\boldsymbol{u}) \\
&= R_{nl}(u)\sum_{m'=-l}^{l} Y_{lm'}(u_\vartheta, u_\varphi) \\
&\quad \times D^l_{m'm}(q_\alpha, q_\vartheta, q_\varphi).
\end{aligned} \tag{A.5}$$

The complex factors $D^l_{m'm}(q_\alpha, q_\vartheta, q_\varphi)$ are the matrix elements of the operator $\mathcal{D}(q_\alpha, q_\vartheta, q_\varphi)$ corresponding to the spherical harmonics, i.e.,

$$D^l_{m'm}(q_\alpha, q_\vartheta, q_\varphi) = \langle lm'|\mathcal{D}(q_\alpha, q_\vartheta, q_\varphi)|lm\rangle. \tag{A.6}$$

Since the final expressions do not depend on q_α, it is possible to include an additional integral $\frac{1}{2\pi}\int \mathrm{d}q_\alpha$. Making use of the properties of the matrices $D^l_{m'm}$ [8], we can easily evaluate the integrals over q_ϑ and q_φ. The arising matrix elements of the form

$$\begin{aligned}
\langle nlm|e^{iaz}|n'l'm\rangle &= \int \mathrm{d}\boldsymbol{r}\, R_{nl}(r)R_{n'l'}(r)e^{iar\cos\vartheta} \\
&\quad \times Y^*_{lm}(\vartheta, \varphi)Y_{l'm}(\vartheta, \varphi)
\end{aligned} \tag{A.7}$$

are calculated using Mathematica.

The evaluation of the integral over q is straightforward. At first, we interchange the integral over q with the integral belonging to the principal value in Eq. (13). Then we treat the arguments of the delta functions in Eqs. (12) and (13) as functions of q and use the relation

$$\delta\left(f\left(q\right)\right) = \sum_i \left| \left.\frac{\partial f}{\partial q}\right|_{q=q_i} \right|^{-1} \delta\left(q - q_i\right), \tag{A.8}$$

where the sum is over all roots q_i of $f\left(q\right)$.

The final task is the evaluation of the integral with the pricipal value in $\Delta_{\nu\nu'\mathbf{0}}\left(\omega\right)$. This will be done numerically using Hartree units. One can read from the delta functions obtained by using Eq. (A.8) for which energies E there will be a contribution to the integral. According to the values of the material parameters of Cu_2O the maximum and minimum value of E are given by

$$E_{\max} \;=\; R_{\mathrm{exc}} + \hbar\omega_{\mathrm{LO},\,\max} > 0, \tag{A.9a}$$

$$E_{\min} \;=\; -E_{\max} - \frac{\hbar^2 q_{\max}^2}{2M} < 0, \tag{A.9b}$$

where $\hbar\omega_{\mathrm{LO},\,\max}$ denotes the energy of the LO-phonon mode with highest energy. Since $\left|E_{\min}\right| > E_{\max}$ holds, we can replace the upper value of the integral by $-E_{\min}$ and rewrite the principal value integral as an improper integral

$$\mathcal{P}\int_{E_{\min}}^{-E_{\min}} \mathrm{d}E\, f\left(E\right) = \lim_{\epsilon\to 0}\int_{\epsilon}^{-E_{\min}} \mathrm{d}E\, \left(f\left(E\right) + f\left(-E\right)\right), \tag{A.10}$$

which is then evaluated using Gaussian quadrature and a standard algorithm for improper integrals.

[1] J. Frenkel, Phys. Rev. **37**, 17 (1931).
[2] J. Frenkel, Phys. Rev. **37**, 1276 (1931).
[3] J. Frenkel, Phys. Z. Sowjetunion **9**, 533 (1936).
[4] R. Peierls, Annalen der Physik **405**, 905 (1932).
[5] G. Wannier, Phys. Rev. **52**, 191 (1937).
[6] E. Gross and I. Karryjew, Dokl. Akad. Nauk. SSSR **84**, 471 (1952).
[7] R. Elliott, in *Polarons and Excitons*, edited by C. Kuper and G. Whitefield (Oliver and Boyd, Edinburgh, 1963), pp. 269–293.
[8] R. Knox, *Theory of excitons*, vol. 5 of *Solid State Physics Supplement* (Academic, New York, 1963).
[9] R. Knox and D. Dexter, *Excitons* (Wiley, New York, 1981).
[10] T. Kazimierczuk, D. Fröhlich, S. Scheel, H. Stolz, and M. Bayer, Nature **514**, 343 (2014).
[11] F. Schöne, S.-O. Krüger, P. Grünwald, M. Aßmann, J. Heckötter, J. Thewes, D. Fröhlich, M. Bayer, H. Stolz, and S. Scheel, arXiv:1511.05458 (2015).
[12] M. Aßmann, J. Thewes, D. Fröhlich, and M. Bayer (to be published).
[13] J. Thewes, J. Heckötter, T. Kazimierczuk, M. Aßmann, D. Fröhlich, M. Bayer, M. A. Semina, and M. M. Glazov, Phys. Rev. Lett. **115**, 027402 (2015).
[14] M. Feldmaier, J. Main, F. Schweiner, H. Cartarius, and G. Wunner (to be published).
[15] Y. Toyozawa, J. Phys. Chem. Solids **25**, 59 (1964).
[16] G. M. Kavoulakis, Y.-C. Chang, and G. Baym, Phys. Rev. B **55**, 7593 (1997).
[17] C. Uihlein, D. Fröhlich, and R. Kenklies, Phys. Rev. B **23**, 2731 (1981).
[18] Y. Toyozawa, Prog. Theor. Phys. **20**, 53 (1958).
[19] Y. Toyozawa, Suppl. Prog. Theor. Phys. **12**, 111 (1959).
[20] Y. Toyozawa, Prog. Theor. Phys. **27**, 89 (1962).
[21] K. Shindo, T. Goto, and T. Anzai, J. Phys. Soc. Jpn. **36**, 753 (1974).
[22] U. Rössler, *Solid State Theory* (Springer, Berlin, 2009), 2nd ed.
[23] J. Bardeen and W. Shockley, Phys. Rev. **80**, 72 (1950).
[24] H. Fröhlich, Advances in Physics **3**, 325 (1954).
[25] O. Madelung and U. Rössler, eds., *Landolt-Börnstein*, vol. 17 a to i, 22 a and b, 41 A to D of *New Series, Group III* (Springer, Berlin, 1982-2001).
[26] J. Hodby, T. Jenkins, C. Schwab, H. Tamura, and D. Trivich, J. Phys. C: Solid State Phys. **9**, 1429 (1976).
[27] T. Ohyama, T. Ogawa, and H. Nakata, Phys. Rev. B **56**, 3871 (1997).
[28] J. Hopfield, J. Phys. Chem. Solids **22**, 63 (1961).
[29] L. Zverev, M. Noskov, and M. Shur, Soviet Phys.- Solid State **2**, 2357 (1961).
[30] J. Grun and S. Nikitine, J. Phys. France **24**, 355 (1963).
[31] S. Rudin, T. L. Reinecke, and B. Segall, Phys. Rev. B **42**, 11218 (1990).
[32] S. Nikitine, J. Grun, and M. Sieskind, J. Phys. Chem. Solids **17**, 292 (1961).
[33] S. Nikitine and R. Reiss, J. Phys. Chem. Solids **16**, 237 (1960).
[34] R. Elliott, Phys. Rev. **108**, 1384 (1957).
[35] P. Yu and Y. Shen, Phys. Rev. B **12**, 1377 (1975).
[36] K. Huang, Zeitschrift für Physik **171**, 213 (1963).
[37] C. Carabatos, phys. stat. sol. (b) **37**, 773 (1970).
[38] C. Carabatos and B. Prevot, phys. stat. sol. (b) **44**, 701 (1971).
[39] M. Beg and S. Shapiro, Phys. Rev. B **13**, 1728 (1976).
[40] C. Klingshirn, *Semiconductor Optics* (Springer, Berlin, 2007), 3rd ed.
[41] A. Jolk and C. Klingshirn, phys. stat. sol. (b) **206**, 841 (1998).
[42] S. Nikitine, in *Optical Properties of Solids*, edited by S. Nudelman and S. Mitra (Springer Science and Busi-

ness Media, New York, 1969), pp. 197–238.
[43] U. Fano, Phys. Rev. **124**, 1866 (1961).
[44] T. Ueno, J. Phys. Soc. Jpn. **26**, 438 (1969).
[45] K. Hannewald, S. Glutsch, and F. Bechstedt, in *Ultrafast Dynamical Processes in Semiconductors*, edited by K.-T. Tsen (Springer, Berlin, 2004), vol. 92 of *Topics in Applied Physics*, pp. 139–192.
[46] V. Agekyan, B. Monozon, and I. Shiryapov, phys. stat. sol. (b) **66**, 359 (1974).
[47] S. Rudin and T. L. Reinecke, Phys. Rev. B **66**, 085314 (2002).
[48] M. Kanehisa, Physica B+C **117-118**, 275 (1983).
[49] V. Gantmakher and Y. Levinson, *Carrier Scattering in Metals and Semiconductors*, vol. 19 (North-Holland, Amsterdam, 1987).
[50] J. Hallberg and R. Hanson, phys. stat. sol. (b) **42**, 305 (1970).
[51] J. I. Jang and J. P. Wolfe, Phys. Rev. B **73**, 075207 (2006).
[52] V. Agekyan, phys. stat. sol. (a) **43**, 11 (1977).
[53] J. Merle, S. Nikitine, and H. Haken, phys. stat. sol. (b) **61**, 229 (1974).
[54] A. Mitchell and M. Zemansky, *Resonance Radiation and Excited Atoms* (Cambridge University Press, Cambridge, 1971).
[55] A. K. Viswanath, J. I. Lee, D. Kim, C. R. Lee, and J. Y. Leem, Phys. Rev. B **58**, 16333 (1998).
[56] J. Dahl and A. Switzendick, J. Phys. Chem. Solids **27**, 931 (1966).
[57] G. Dasbach, D. Fröhlich, R. Klieber, D. Suter, M. Bayer, and H. Stolz, Phys. Rev. B **70**, 045206 (2004).
[58] A. Messiah, *Quantenmechanik*, vol. 1 (Walter de Gruyter, Berlin, 1976).
[59] A. Edmonds, *Angular momentum in quantum mechanics* (Princeton University Press, Princeton, 1960).